Sigma J Eng & Nat Sci 37 (3), 2019, 903-916

Sigma Journal of Engineering and Natural Sciences
Sigma Mühendislik ve Fen Bilimleri Dergisi

Research Article

NUMERICAL MODELLING OF SUDDEN CONTRACTION IN PIPE FLOW

Engin GÜCÜYEN*[1], Recep Tuğrul ERDEM[2], Ümit GÖKKUŞ[3]

[1]*Manisa Celal Bayar University, Department of Civil Engineering, MANISA;* ORCID: 0000-0001-9971-8546
[2]*Manisa Celal Bayar University, Department of Civil Engineering, MANISA;* ORCID: 0000-0002-8895-7602
[3]*Manisa Celal Bayar University, Department of Civil Engineering, MANISA;* ORCID: 0000-0002-2422-6392

Received: 31.01.2019 Revised: 03.05.2019 Accepted: 14.06.2019

ABSTRACT

In the present work, full-scale numerical simulations of incompressible fluid flow through different locations of sudden contractions are studied according to Computational Fluid Dynamics (CFD) technique. Finite Elements Method is used to numerically solve governing equations via the commercial program ABAQUS including CFD code. Four different locations of contraction zone are utilized to determine the effect of location changes on sudden contraction head loss coefficients (K_C). Twelve area ratios (σ) are performed for all zones. Three different Reynolds numbers, remain in laminar flow boundaries, are adopted to determine effects of Reynolds number, as well as location effects. The graphs are constituted by results from computing 48 models for each Reynolds number and the study is concluded with 144 models in the end. In this manner, contraction ratio varying coefficients are obtained for four configurations. According to results, the pressure drop values of the same model for varying contraction locations are different. Maximum values of pressure drops are obtained for the second geometry (G_2). Combination of maximum pressure drops and minimum velocity values leads to maximum contraction coefficients for G_2. While the area coefficients increase, decreasing values of contraction coefficients of different contraction locations (G) converge in connection with the changing values of velocities and pressure drops. It is necessary to entrain to this remark, for increasing area coefficients. It is stated that K_C-σ curves vary due to location change. It is recommended to consider the location varying coefficients while modelling different located contracting flows especially for side contracting flows.
Keywords: Sudden contraction coefficients, contraction location effects, computational fluid dynamics, finite elements.

1. INTRODUCTION

Sudden contraction applications are widely used in different fields of engineering including civil, nuclear, mechanical, chemical, pharmaceutical, food, bio and biomedical. Contraction or expansion problems are only ceased to be the subject of civil and mechanical engineering by developing multi-disciplinary engineering approaches such as bio engineering. As an example, a sudden contraction of a blood vessel has started to be studied by likened pipe flow [1, 2, 3].

Cross section area of pipe flow may change according to sediment erosion, the location, fluid pipe transports and intended purpose. If the change in pipe cross-section is gradual, no flow

* Corresponding Author: e-mail: engin.gucuyen@cbu.edu.tr, tel: (236) 201 23 21

separation occurs and the c hange of static pressure may effectively convert to the kinetic energy. However, if there is a sudden change in the flow area, it may cause a significant loss due to additional turbulence arising in the connection [4-11]. Each type of loss can be quantified by using a loss coefficient (K_C). Velocity of flow and geometry of device directly effect the amount of losses. A significant amount of pressure drop occurs due to sudden contraction in pipe by increasing the velocity and the losing energy.

The changes are encountered as contraction or expansion. In this study, contraction problem is deeply investigated. The simple geometrical configuration of contracting flow is formed by two pipes having different diameters [13]. As well as this simple form, more complex coaxially form can be seen in connected pipes of different diameters. Coaxial contraction will be separately located at the side, at the top [14], and the bottom [6]. One co axial and three with coaxial scenarios that are studied in this paper are seen in Figure 1. The diameter ratio of inlet to outlet pipe is taken as the main geometric parameter which is referred to as the area ratio, (σ) [15, 16].

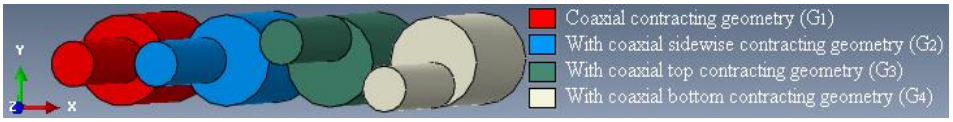

Figure 1. Geometrical models in analyses

Its geometrical simplicity and hydrodynamic complexity make sudden contraction as an ideal problem for testing various numerical methods. As a result, a wealth of literature exists on such a flow covering a wide range of fluids and governing parameters. In addition to other methods such as Finite Volume Method [11, 17, 18], Finite Elements Method can be implemented in numerical studies as utilized in this study [19, 20, 21].

This study is aimed at determining contraction location on sudden contraction coefficients which is called (K_C). For this purpose, four geometrical scenarios are set out including one co axial and three with coaxial sudden contracting geometries. In the modelling phase, twelve different diameter ratios of outlet to inlet of the pipe are utilized for all geometries. As a result, forty-eight geometries are modelled in total. The models under consideration have undergone three inlet velocities to determine Reynolds number effects as well as location effects. ABAQUS [22] Finite Elements Analysis program is used to perform analyses. It is seen that K_C values that are obtained after analysis are compatible with the previous studies in the literature [23, 24].

2. NUMERICAL STUDY

A numerical investigation into the effect of contraction location changes on the sudden contraction coefficients of single-phase flow in full-scale models has been conducted in this paper. In the first stage of the study, geometrical models are generated to evaluate the numerical analyses. According to the results which are obtained from analyses, the contraction coefficients are calculated and effects of location on sudden contraction coefficients are determined.

2.1. Geometrical Models

In this study, four geometrical configurations each of them including twelve contraction ratios are investigated. First configuration is commonly used as coaxial contracting flow. In this configuration, both normal axis (z) of inlet and outlet flow are located in the same axis. The other configurations are formed as with coaxial contracting flows. The normal axis of inlet and outlet flows is not randomly located. With coaxial contracting configurations are composed of side, top and bottom ones are contracting models. The sudden contraction geometries consist of two pipes. While the first one is inlet, the other one is outlet. Inlet flow diameter (D) is maintained constant

throughout this study and it is equal to 1 m. Outlet flow diameters (*d*) vary between 0.30 and 0.85 with 0.05 increments as given in Table 1.

Table 1. Diameters of inlet and outlet pipes

D (m)	1.00	1.00	1.00	1.00	1.00	1.00	1.00	1.00	1.00	1.00	1.00	1.00
d (m)	0.30	0.35	0.40	0.45	0.50	0.55	0.60	0.65	0.70	0.75	0.80	0.85
σ	0.090	0.123	0.160	0.203	0.250	0.303	0.360	0.423	0.490	0.563	0.640	0.723

The values which are taken from well-known contraction coefficient graphic [24] have been utilized to calculate area ratios (σ). This ratio is the geometry range that is defined by the contraction area ratio from outlet (A_d) to inlet (A_D) corresponding to the diameter d and D respectively.

Figure 2.a. Co axial contracting flow geometries (G_1)

Figure 2.b. With co axial side contracting flow geometries (G_2)

Figure 2.c. With co axial top contracting flow geometries (G_3)

Figure 2.d. With co axial bottom contracting flow geometries (G_4)

The geometries modelled in the program are seen in Figures 2.a-d. Twelve diameter ratios are adopted to realize flow scenarios for all geometries. The ratios are starting with 0.09 and ending with 0.73 by selecting the diameters from 0.3 to 0.85. As a result, forty-eight geometries are modelled by ABAQUS to determine location effects on sudden contraction ratios.

2.2. Description of Numerical Computations and Boundary Conditions

In this study, the utilized numerical approach is based on the numerical solution of the steady, incompressible mass conservation and momentum equations given by Eqs.(1-4). Finite elements method (FEM) is adopted to evaluate these equations.

$$\frac{\partial}{\partial x}(\rho u)+\frac{\partial}{\partial y}(\rho v)+\frac{\partial}{\partial z}(\rho w)=0 \tag{1}$$

$$\frac{\partial u}{\partial t}+\frac{\partial}{\partial x}(\rho u^2)+\frac{\partial}{\partial y}(\rho uv)+\frac{\partial}{\partial z}(\rho uw)=-\frac{\partial P}{\partial x}+\mu\left(\frac{\partial^2 u}{\partial x^2}+\frac{\partial^2 u}{\partial y^2}+\frac{\partial^2 u}{\partial z^2}\right) \tag{2}$$

$$\frac{\partial v}{\partial t}+\frac{\partial}{\partial x}(\rho uv)+\frac{\partial}{\partial y}(\rho v^2)+\frac{\partial}{\partial z}(\rho vw)=-\frac{\partial P}{\partial y}+\mu\left(\frac{\partial^2 v}{\partial x^2}+\frac{\partial^2 v}{\partial y^2}+\frac{\partial^2 v}{\partial z^2}\right) \tag{3}$$

$$\frac{\partial w}{\partial t}+\frac{\partial}{\partial x}(\rho uw)+\frac{\partial}{\partial y}(\rho vw)+\frac{\partial}{\partial z}(\rho w^2)=-\frac{\partial P}{\partial z}+\mu\left(\frac{\partial^2 w}{\partial x^2}+\frac{\partial^2 w}{\partial y^2}+\frac{\partial^2 w}{\partial z^2}\right) \tag{4}$$

In Eqs.(1-4) u, v and w are the velocity components at the x, y and z coordinate directions respectively. ρ, μ and P stand for the density, the dynamic viscosity and the pressure. In this study, the fluid is incompressible and Newtonian. The regime is stationary. The used fluid is water, at temperature of 20 $C°$. The other properties are used as follows: ρ=988.2 kg/m^3 and μ=1004.10^{-6} m^2/s. Average velocity values of 0.80 m/s, 1.20 m/s and 1.60 m/s have been used as normal uniform velocity inlet boundary condition in this work. In this manner, effect of Reynolds number on contraction coefficient can be seen. The velocity at the inlet is parallel to the inlet flow axis without cross stream components [24]. Zero pressure value and no streamwise variation for velocity components have been set at the outlet boundary. At the remaining domain surfaces are set non-slip wall boundary conditions. The boundary conditions that are described above, can be mathematically represented in Table 2. [19]. Eqs.(1-4) are solved abiding the boundary conditions via [22].

Table 2. Boundary conditions

Surfaces	Boundary Conditions
Inlet	$u\neq0$, $v=w=0$
Outlet	$P=0$, $\partial u/\partial x+\partial v/\partial x+\partial w/\partial x=0$
Non-slip walls	$u=v=w=0$

The geometry of the second configuration is illustrated in Figure 3 with boundary conditions on it. The considered models which are horizontally located are shown below.

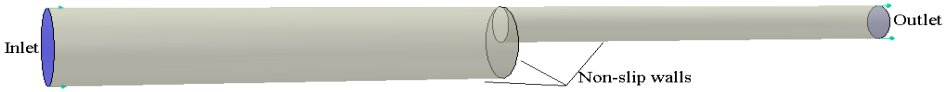

Figure 3. The geometry of the third configuration (G_3) and boundary conditions

2.3. Mesh Design and Sensivity Analyses

Velocity and pressure values shall be calculated to obtain loss coefficients. For this purpose, ABAQUS program which is widely used by researchers for dynamic analyses is performed for solutions [26]. First of all, forty eight flow geometries including co-axial and with co-axial sudden contracting flow geometries are modelled in the program. The utilized flow properties have been mentioned in the previous section. FC3D4 (4-node modified tetrahedron) typed members which are proper for CFD problems are used in the analyses. Before performing analyses, mesh independence test should be performed as far as the solutions have become closer

for different mesh sizes. This test is executed for average axial outlet velocities of one model. A series of simulations are firstly carried out for the outlet diameter (*d*) 0.30 m for co-axial geometry. Test is performed on four mesh configurations with different levels of refinement, as shown in Figures 4.a-d respectively. Perfective and cross-section wives of nodes used for Finite Element Analysis are seen in figures below.

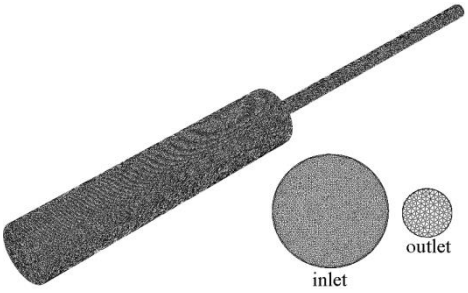

Figure 4.a. Wives of node 1

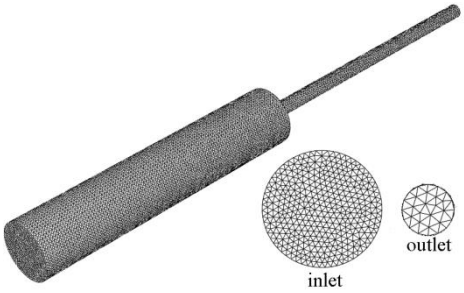

Figure 4.b. Wives of node 2

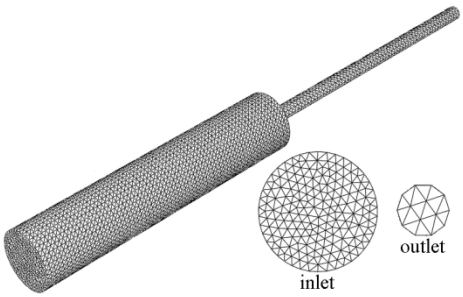

Figure 4.c. Wives of node 3

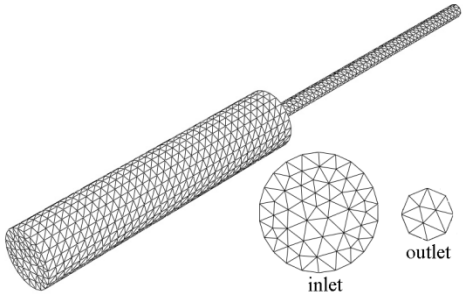

Figure 4.d. Wives of node 4

Distances between meshes are taken as 0.010 m, 0.025 m, 0.05 m and 0.075 m for the nodes 1-4 respectively to determine the mesh results. 133684 nodes and 703438 elements constitute Node 1, 27407 nodes and 138384 elements constitute node 2, 10658 nodes and 52222 elements constitute node 3, 4951 nodes and 22987 elements constitute node 4. For 0.8 m/s inlet velocity, average axial velocity values of 8.8293 m/s, 8.9163 m/s, 9.5995 m/s and 10.2771 m/s are acquired for nodes 1-4 respectively. As it is inferred from the values that are given above, the results are closer while the distance between meshes are adopted between 0.010 and 0.025. While minimizing the size of elements, analyses duration lengthens out and analyses increase in volume simultaneously. For this reason, 0.025 m distances between meshes are performed in the analysis for all models and ultimate mesh structure is formed in the end.

3. NUMERICAL RESULTS AND CALCULATION OF SUDDEN CONTRACTION COEFFICIENTS

When a single-phase fluid flows through a sudden contraction, the mechanical energy loss takes place predominantly during the deceleration following the vena-contracta point *C* as shown in Figure 5 [27].

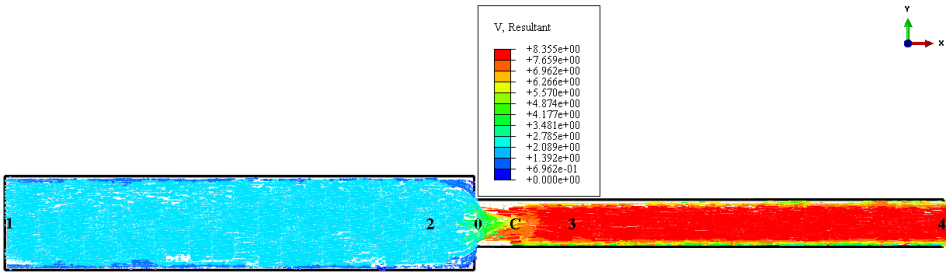

Figure 5. Velocity contours and pressure points of σ_5 for Re=1600

The figure demonstrates the velocity vectors of coaxial contracting flow (σ_5) with Reynolds number of 1600. The schemes of pressure locations are evaluated to calculate loss coefficients (K_C) as given by Eqs. (5-7), are approximately valid for all geometries.

$$\Delta P_C = \Delta P_{23} - \frac{\Delta P_{34} L_{03}}{L_{34}} - \frac{\Delta P_{12} L_{02}}{L_{12}} - \Delta P_{PR} \tag{5}$$

$$\Delta P_{PR} = \rho u_D^{\,2} (2 - \sigma^2) / 2 \tag{6}$$

$$K_C = 2\Delta P_C / \rho u_d^{\,2} (2 - \sigma^2) \tag{7}$$

The loss is related to the velocity (u_D) in the outlet pipe, area ratio (σ), density (ρ) and sudden pressure change due to contraction (ΔP_C). Combination of the pressure drop (ΔP_{34}) between points 4-3, the friction pressure drop in the straight pipe, the pressure drop Δ_{PR} due to the change in velocity, and Δ_{PC} forms the pressure drop (ΔP_{23}) between points 2 and 3. Distance between points is represented by L [25]. Pressure values of the first area ratio (σ_1=0.09) which are used to obtain loss coefficients are given in Tables 3-6 for increasing Reynolds number. Pressure at the point 4 is set to zero in boundary conditions.

Table 3. Pressure values of σ_1 for Re=800

Re=800	P_1 (Pa)	P_2 (Pa)	P_0 (Pa)	P_C (Pa)	P_3 (Pa)
G_1	31414.31	31405.24	18933.17	2929.94	1272.49
G_2	31567.64	31597.55	16123.33	1523.45	869.78
G_3	31573.97	31384.37	16144.03	1548.09	994.98
G_4	31434.78	31245.07	15956.61	1509.93	793.79

Table 4. Pressure values of σ_1 for Re=1200

Re=1200	P_1 (Pa)	P_2 (Pa)	P_0 (Pa)	P_C (Pa)	P_3 (Pa)
G_1	70598.90	70307.91	36692.12	6553.16	2889.98
G_2	70782.39	70611.32	36116.34	3391.52	1948.33
G_3	70725.69	70301.03	36162.65	3467.72	2228.73
G_4	70413.91	69989.45	35342.83	3398.24	1778.15

Table 5. Pressure values of σ_1 for Re=1600

Re=1600	P_1 (Pa)	P_2 (Pa)	P_0 (Pa)	P_C (Pa)	P_3 (Pa)
G_1	126009.52	125490.2	65490.52	11796.55	5158.23
G_2	125658.32	124904.2	64250.12	6001.09	3459.78
G_3	124074.11	123329.2	63440.17	6083.42	3909.86
G_4	119048.82	120330.4	60430.42	5939.64	3006.24

Although finite elements analyses of all models are performed by Finite Elements Program, results of all models are not given. Only three of them are presented including σ_1, σ_6 and σ_{12} as example solutions. Pressure values of σ_6 are given between Tables 6-8.

Table 6. Pressure values of σ_6 for Re=800

Re=800	P_1 (Pa)	P_2 (Pa)	P_0 (Pa)	P_C (Pa)	P_3 (Pa)
G_1	6501.23	6207.8	3233.6	384.78	181.68
G_2	6571.92	6580.21	2831.65	438.20	185.32
G_3	6645.98	6610.07	3305.48	509.85	229.21
G_4	6751.81	6702.02	3206.68	499.45	212.19

Table 7. Pressure values of σ_6 for Re=1200

Re=1200	P_1 (Pa)	P_2 (Pa)	P_0 (Pa)	P_C (Pa)	P_3 (Pa)
G_1	15129.24	15089.02	7953.89	613.01	270.35
G_2	15318.45	15226.23	7199.89	636.18	358.17
G_3	15354.32	15281.41	7225.91	638.48	410.36
G_4	15311.5	15047.52	7115.25	672.10	383.84

Table 8. Pressure values of σ_6 for Re=1600

Re=1600	P_1 (Pa)	P_2 (Pa)	P_0 (Pa)	P_C (Pa)	P_3 (Pa)
G_1	27239.1	26577.3	14118.1	1105.4	425.07
G_2	26743.62	26735.90	11876.10	994.75	432.0282
G_3	27802.83	27791.30	13742.60	1215.31	694.0647
G_4	27855.47	27688.20	13651.80	1112.23	650.5676

The pressure values at certain nodes for σ_{12} are given between Table 9 and Table 11 for increasing Re number.

Table 9. Pressure values of σ_{12} for Re=800

Re=800	P_1 (Pa)	P_2 (Pa)	P_0 (Pa)	P_C (Pa)	P_3 (Pa)
G_1	1451.45	1451.03	721.12	72.35	31.42
G_2	1461.26	1452.44	741.75	65.54	36.92
G_3	1451.89	1451.28	741.56	70.04	40.04
G_4	1452.49	1443.76	742.67	71.21	45.77

As it can be easily understood from Eq. (7), not only pressure drops but also velocity values are effective on sudden contraction coefficients. Therefore, velocity values should also be given. In terms of referring to different samples, results of σ_2 and σ_{10} which have not taken part in previous figures are given between Figures 6-13. The flow geometries are vertically cut in vertical axis (y), as it is in the middle of contraction region. Unlike other geometries, there is a need to give all views of G_2 because of having unsymmetrical contraction location.

Table 10. Pressure values of σ_{12} for Re=1200

Re=1200	P_1 (Pa)	P_2 (Pa)	P_0 (Pa)	P_C (Pa)	P_3 (Pa)
G_1	3281.62	3262.80	1666.29	147.23	82.89
G_2	3417.34	3414.92	1746.45	164.96	94.21
G_3	3367.36	3366.39	1672.99	167.85	72.89
G_4	3353.86	3332.72	1714.85	164.87	105.68

Table 11. Pressure values of σ_{12} for Re=1600

Re=1600	P_1 (Pa)	P_2 (Pa)	P_0 (Pa)	P_C (Pa)	P_3 (Pa)
G_1	7419.49	7376.94	3767.36	332.87	187.40
G_2	7991.87	7986.22	4084.29	385.78	220.33
G_3	7809.89	7807.65	3880.15	389.29	169.05
G_4	7744.20	7695.39	3959.66	380.69	244.01

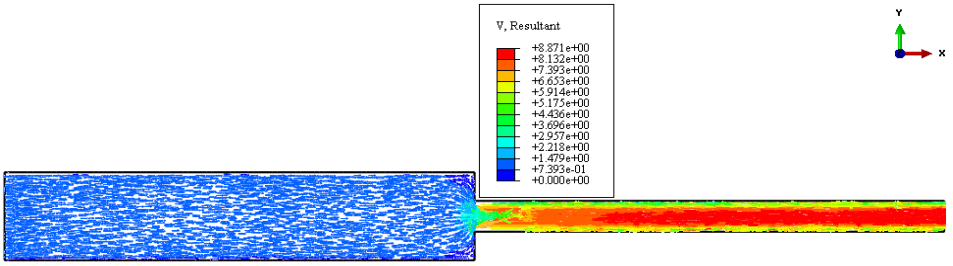

Figure 6. Velocity values of σ_2- G_1 for Re=800

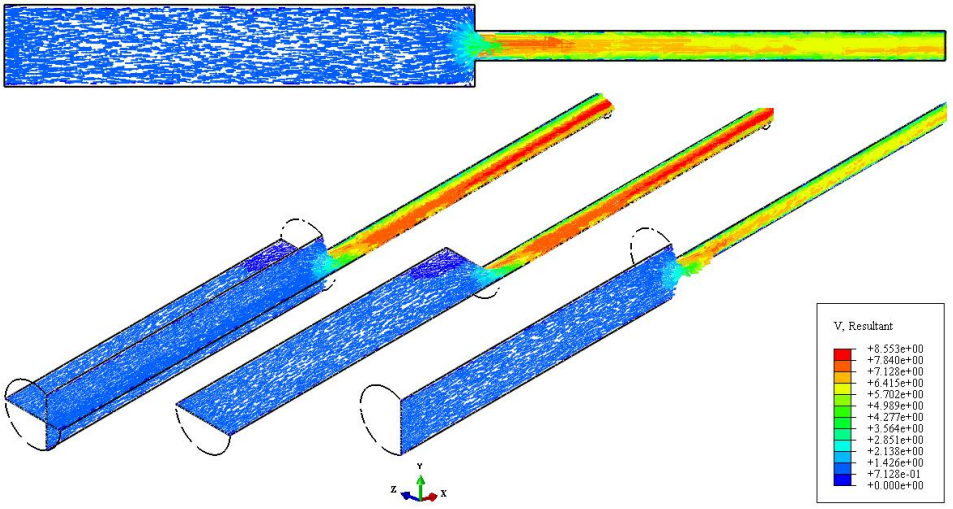

Figure 7. Velocity values of σ_2- G_2 for Re=800

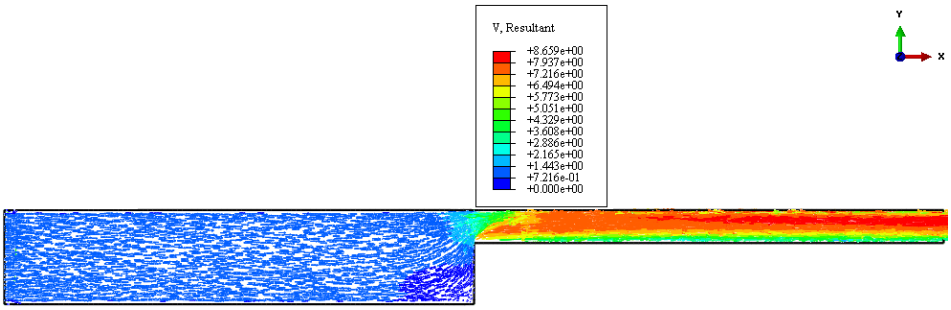

Figure 8. Velocity values of σ_2- G_3 for Re=800

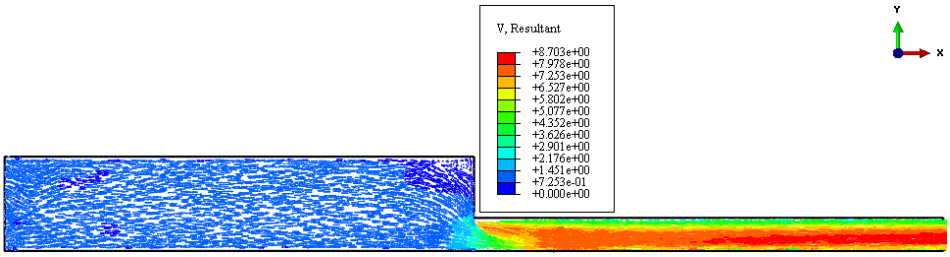

Figure 9. Velocity values of σ_2- G_4 for Re=800

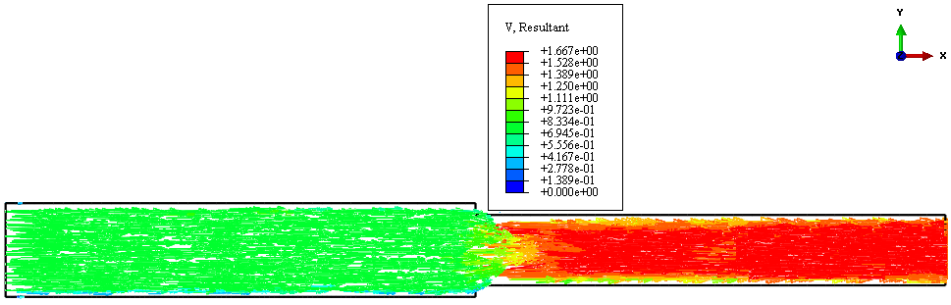

Figure 10. Velocity values of σ_{10}- G_1 for Re=800

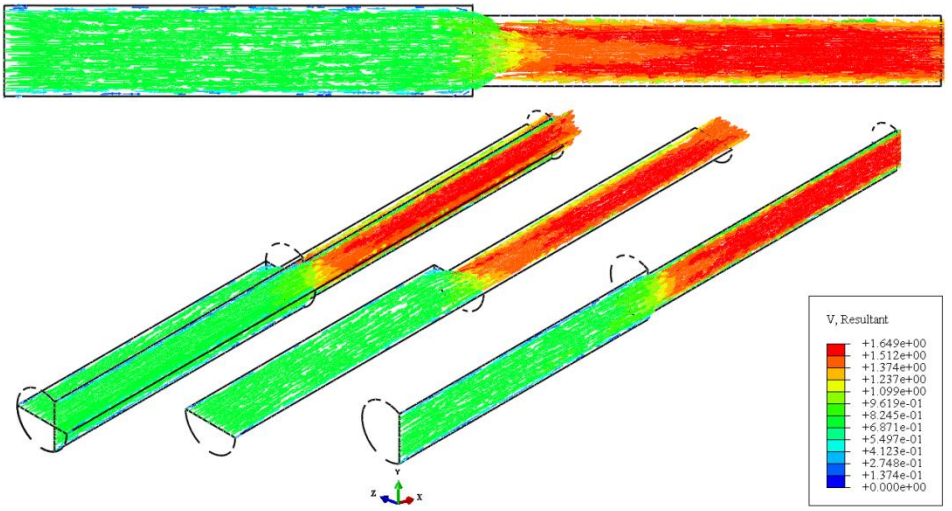

Figure 11. Velocity values of σ_{10}- G_2 for Re=800

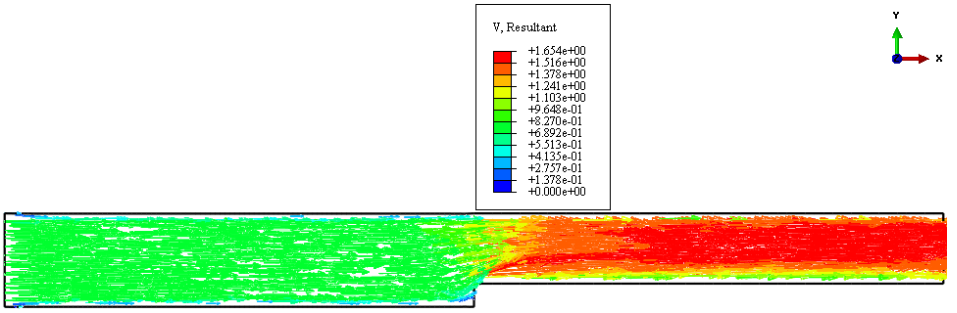

Figure 12. Velocity values of σ_{10}- G_3 for Re=800

Velocity values presented in the figures above and pressure values given in tables are evaluated to calculate loss coefficients of sudden contracting pipe flow. The graphs of sudden contraction coefficients are given in Figures 14.a-c for three different Re numbers to detect effects on coefficients. Three different Reynolds numbers that remain in laminar flow boundaries are adopted to determine effects of Reynolds number, as well as location effects. The graphs are constituted by the results from computing 48 models for each Reynolds number and the study is concluded with 144 models in the end.

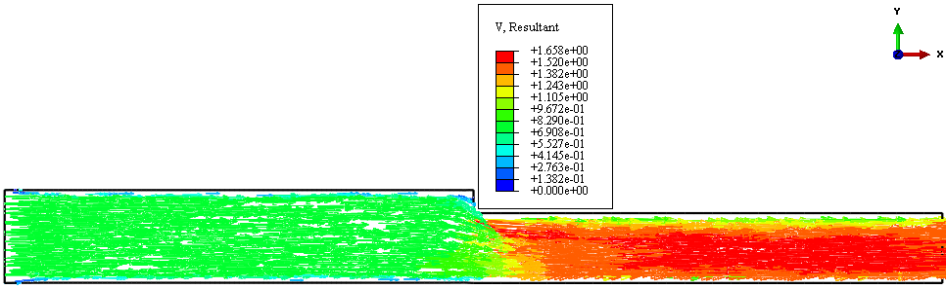

Figure 13. Velocity values of σ_{10}- G_4 for Re=800

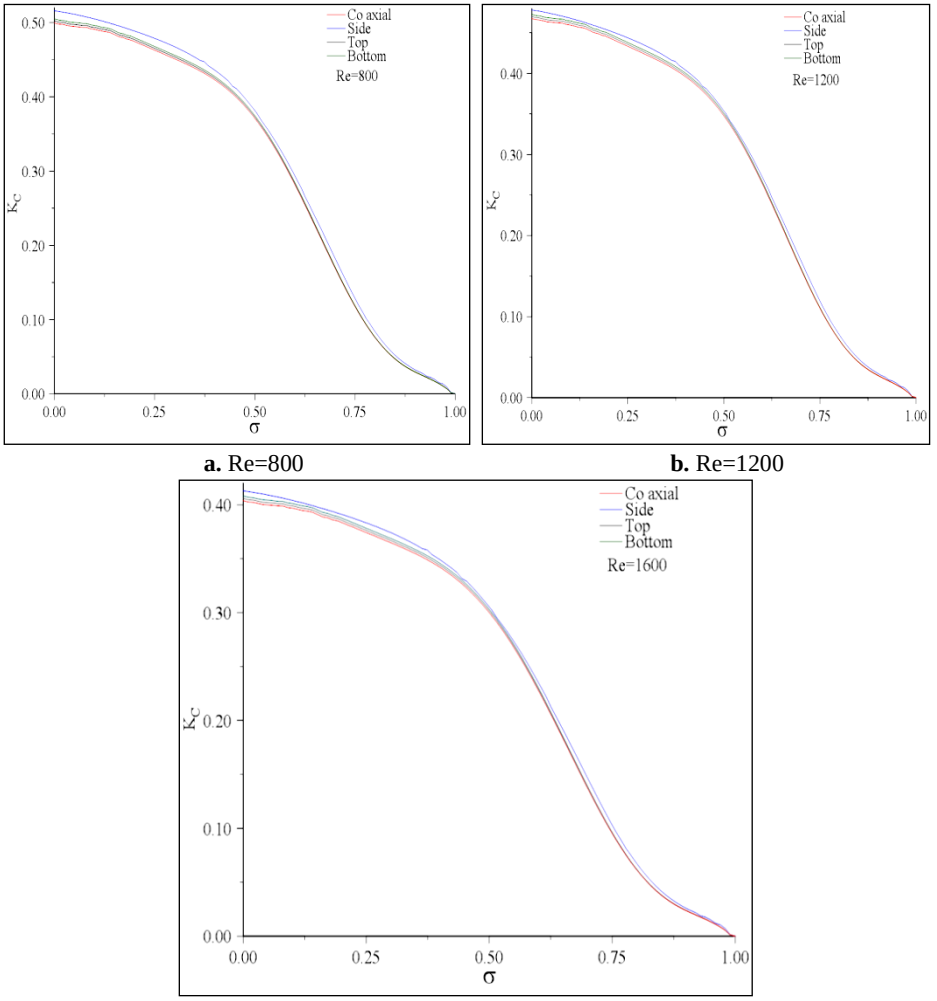

a. Re=800 **b.** Re=1200

c. Re=1600

Figure 14. Varying sudden contraction coefficients with Reynolds numbers

It is known from the previous studies in the literature that values of contraction head loss coefficients vary between 0.00 and 0.50. It is presented in Figure 14 that obtained results after numerical analyses remain between the expected values.

4. CONCLUSIONS

In this paper, it is aimed to detect effects of changes of contraction locations on sudden contraction coefficients. In order to determine these efxfects, large scaled specimens including 48 models are numerically studied and analysed via ABAQUS. While performing the regular analyses, the sensitivity analyses are carried out simultaneously. Node distances are determined as 0.025 m according the sensitivity analyses.

The contraction coefficients are directly effected by three parameters; area ratios, velocity and pressure drop respectively. While an inlet and outlet narrowing flow geometries are connected, increase in velocity and energy losses occur and this situation induces drop of pressure. In previous studies, the effects of varying area ratios and velocities on contraction coefficients have already been studied. But it is known that, the outlet pipe will be connected to different locations of inlet pipe such as at the side, top and bottom. In this study, effect of location changes on contraction coefficients are examined by means of Figures 6-13 and Tables 3-11. These results are obtained from only a portion of 144 models. The graph covering all of the model results is given in Figure 14. In this figure, both Reynolds number and area ratio varying loss coefficients are presented.

Although having the same boundary conditions and mesh structure same model (σ) produce different velocity values for different contraction locations (G). The outlet velocity values adopted to calculate coefficients are given between Figures 6-9 for σ_2 and between Figures 10-13 for σ_{10} in which Re is 800. While the values of σ_2 are 8.871 m/s, 8.553 m/s, 8.659 m/s and 8.703 m/s, the values of σ_{10} are 1.667 m/s, 1.649 m/s, 1.654 m/s and 1.658 m/s for G_1, G_2, G_3 and G_4 respectively. Minimum value is obtained for side contracting with coaxial flow and the maximum one is obtained for coaxial contracting flow for both models. The difference brings out the contraction location between minimum and maximum values is 3.58% for σ_2 and 1.02% for σ_{10}. The results reveal that the differences between outlet velocity values of the models decrease unlike the increase in σ. Same situation is observed for all models mentioned in this study. The difference approximately reverberates on contraction coefficients regarding the differences of drop of pressure. The analyses have been performed for increasing Re number and it is stated that the loss coefficient is decreasing for increasing Re numbers, as it has been mentioned in previous studies.

Based on the results given in Tables 3-11, one can easily indicate that drop of pressure values of the same model for varying contraction locations are different. According to mentioned tables, maximum values of pressure drops are obtained for G_2. Combination of maximum drop of pressure, minimum velocity values leads to obtain maximum contraction coefficients for G_2. While the area coefficients increase, decreasing values of contraction coefficients of different contraction locations (G) converge are seen in Figures 14.a-c, due to converging values of velocities and drop of pressure. It is necessary to entrain to this remark, for increasing area coefficients.

It is determined that values of contraction head loss coefficients are approximately same with the general used values. In addition to this, new values are obtained in case of contraction in different locations. New values that are obtained from different locations are close to the values obtained from co axial contraction. These values have been presented by figures and tables in the study. This situation is the main reason of using co axial contraction coefficient in case of different location contraction in practice.

Although not being mentioned in past studies, with coaxial contracting models are widely used in industrial applications which are the starting point of this study. The results predicate this

starting point. It is recommended to take into consideration the location varying coefficients while modelling different located contracting flows especially for side contracting flows. The approach of this study will be implementing to sudden expansion problems for further studies.

5. NOTATION

A_D	(m^2)	Inlet flow cross-section area
A_d	(m^2)	Outlet flow cross-section area
D	(m)	Inlet flow diameter
d	(m)	Outlet flow diameter
G	(1)	Contraction location
K_C	(1)	Loss coefficients
L	(m)	Distance between points
P	(Pa)	Pressure
Re	(1)	Reynolds number
u	(m/s)	Velocity components at the x direction
v	(m/s)	Velocity components at the y direction
w	(m/s)	Velocity components at the z direction
ΔP	(Pa)	Pressure drop
μ	(m^2/s)	Dynamic viscosity
ρ	(kg/m^3)	Density
σ	(1)	Area ratio

REFERENCES

[1] Oliveira P. J., Pinho F. T., and Schulte A., (1998) A General Correlation for the Local Loss Coefficient in Newtonian Axisymmetric Sudden Expansions, *International Journal of Heat and Fluid Flow* 19, 655-660.

[2] Nillesen S. T. M., Lammers G., Wismans R. G., Ulrich M. M., Middelkoop E., Spauwen P. H., Faraj K. A., Schalkwijk J., Daamen W. F., and Van Kuppevelt T. H., (2011) Design and in Vivo Evaluation of a Molecularly Defined a Cellular Skin Construct: Reduction of Early Contraction and Increase in Early Blood Vessel Formation, *Acta Biomaterialia* 7, 1063-1071.

[3] Wang X-K., Wang Y-G., Zhan H-L, Chai Y-S., Hu J., Xing D-M., You X-F., Lei F., and Du L-J., (2011) Comprehensive Study of Evodia Rutaecarpa-Induced Contraction on Blood Vascular in Vivo And in Vitro, *Chinese Journal of Natural Medicines*, vol. 9, no. 1, pp. 65-73.

[4] Yan B. H., and Gu H.Y., (2013) Effect of rolling motion on the expansion and contraction loss coefficients, *Annals of Nuclear Energy,* vol. 53, pp, 259-266.

[5] Lewis J. M., and Wang Y., (2018) Investigating the Pressure Loss Associated with Two-Phase Flow in a Rectangular Microchannel Suddenly Expanding into a Manifold, *International Journal of Hydrogen Energy* 43 (36), 17444-17460.

[6] Gücüyen E., Erdem R. T., and Gökkuş Ü., (2016) FSI Analysis of Submarine Outfall, *Brodogradnja/Shipbuilding*, 67(2), 67-80.

[7] Dehkordi P. B., Azdarpour A., and Mohammadian E., (2018) The hydrodynamic behavior of high viscous oil-water flow through horizontal pipe undergoing sudden expansion-CFD study and experimental validation, *Chemical Engineering Research and Design* 139, 144-161.

[8] Colombo L. P. M., Guilizzoni M., Sotgia G. M., and Marzorati D., (2015) Influence of Sudden Contractions on in Situ Volume Fractions for Oil–Water Flows in Horizontal Pipes, *International Journal of Heat and Fluid Flow* 53, 91-97.

[9] Bae Y., and Kim, Y.I., (2014) Prediction of Local Loss Coefficient for Turbulent Flow in Axisymmetric Sudden Expansions with a Chamfer: Effect of Reynolds Number, *Annals of Nuclear Energy* 73, 33-38.

[10] Javadi A., and Nilsson H., (2015) LES and DES of Strongly Swirling Turbulent Flow Through a Suddenly Expanding Circular Pipe, *Computers & Fluids* 107, 301-313

[11] Badr H. M., Habib M. A., Ben-Mansour R., and Said, S. A. M., (2005) Numerical Investigation of Erosion Threshold Velocity in a Pipe with Sudden Contraction, *Computers & Fluids* 34, 721–742.

[12] Ala A. A., Tan S., Eltayeb A., Abbati Z., (2019) Experimental Study on Sudden Contraction and Split into the Inlets of Two Parallel Rectangular Jets, *Experimental Thermal and Fluid Science* 104, 272, 283.

[13] Chalfi T. Y., and Ghiaasiaan S. M., (2008) Pressure Drop Caused by Flow Area Changes in Capillaries under Low Flow Conditions, *International Journal of Multiphase Flow* 34, 2-12.

[14] Hammad K. J., and Vradis G. C., (1996) Creeping Flow of a Bingham Plastic Through Axisymmetric Sudden Contractions with Viscous Dissipation, *International Journal of Heat Mass Transfer* 39(8), 1555-1567.

[15] Yesilata B., Öztekin A., and Neti S., (1999) Instabilities in Viscoelastic Flow Through an Axisymmetric Sudden Contraction, *Journal of Non-Newtonian Fluid Mechanics* 85, 35-62.

[16] Yesilata B., Öztekin A., and Neti S., (2000) Non-isothermal viscoelastic flow through an axisymmetric sudden contraction *Journal of Non-Newtonian Fluid Mechanic* 89, 133-164.

[17] Cherrared D., and Filali E. G., (2013) Hydrodynamics and Heat Transfer in Two and Three-Dimensional Minichannels, *Fluid Dynamics and Materials Processing*, 9(2), 127-151.

[18] Holmesa L., Faverob J., and Osswald T., (2012) Numerical Simulation of Three-Dimensional Viscoelastic Planar Contraction Flow Using the Software Open FOAM, *Computers and Chemical Engineering* 37, 64-73.

[19] Lima R. C., Andrade C. R., and Zaparoli E. L., (2008) Numerical Study of Three Recirculation Zones in the Unilateral Sudden Expansion Flow, *International Communications in Heat and Mass Transfer* 35, 1053–1060.

[20] Kaushik V. V. R., Ghosh S., Das G., and Das P. K., (2012) CFD Simulation of Core Annular Flow Through Sudden Contraction and Expansion, Journal of Petroleum Science and Engineering 86–87, 153-164.

[21] Schrecka E., and Schafer M., (2000) Numerical Study of Bifurcation in Three-Dimensional Sudden Channel Expansions, *Computers & Fluids* 29, 583-593.

[22] ABAQUS User's Manual (2010), Version 6.10.

[23] Cengel Y. A., Cimbala J. M., (2014). Fluid Mechanics Fundamentals and Applications, *Mc Graw Hill*, New York, USA.

[24] Shaughnessy E.J., Katz I. M., and Schaffer J. P., (2005) Introduction to Fluid Mechanics, *Oxford University Press, New York, USA.*

[25] Guo B., Langrish T. A. G., and Fletcher D. F., (1998) Simulation of Precession in Axisymmetric Sudden Expansion Flows, *Second International Conference on CFD in the Minerals and Process Industries*, Csıro, Melbourne, Australia.

[26] Gücüyen E., and Erdem R T., (2018) Beton Kazıklı Açık Deniz Yapısının Analizi, *Selçuk Üniversitesi Mühendislik, Bilim ve Teknoloji Dergisi* 6(4), 767-778.

[27] Guo H., Wang L., Yu J., Ye F., Ma C., and Li Z. (2010) Local resistance of fluid flow across sudden contraction in small channels, *Frontiers of Energy and Power Engineering in China*, vol. 4, no. 2, pp. 149-154.